Minimizing Nonproductive Substrate Binding: A New Look at Glucoamylase Subsite Affinities

Sateesh K. Natarajan[‡] and Michael R. Sierks*

Department of Chemical and Biochemical Engineering, University of Maryland Baltimore County, 1000 Hilltop Circle, Baltimore, Maryland 21250

Received April 8, 1997; Revised Manuscript Received August 11, 1997[⊗]

ABSTRACT: A subsite model as proposed by Hiromi [Hiromi, K. (1970) *Biochem. Biophys. Res. Commun. 40,* 1−6] has been applied to various hydrolases including glucoamylase (GA). The model assumes a single enzyme complex, a hydrolytic rate constant which is independent of substrate length, and a rate-limiting hydrolytic step. Recent kinetic studies with GA contradict these assumptions. Here we reevaluate the substrate binding of GA studying the pre-steady-state kinetics with glucose, which is reported here for the first time, and maltose. The association equilibrium constants for glucose and maltose interactions with wild-type and Trp120→Phe GA from *Aspergillus awamori* in H_2O and D_2O buffers were obtained. Kinetic results indicate that a single glucose molecule binds to GA weakly by a single-step mechanism, $E + G_1 \leftrightarrow EG_1$, under the conditions studied. Similar fluorescence intensities of the GA−glucose and GA−maltose complexes, the high tryptophan concentration around subsite 1, crystal structures of various inhibitor complexes, pre-steady-state and steady-state modeling, feasibility of condensation reactions, and other evidence strongly suggest that glucose binds at subsite 1. These results conflict with the high subsite 2 and low subsite 1 affinities obtained using Hiromi's model. Using the substrate association constants for glucose and maltose obtained by pre-steady-state kinetics, the affinity of α-glucose for subsite 1 is shown to be substantially higher than the apparent affinity of glucose for subsite 2. We propose a GA catalytic mechanism whereby substrate binding is initiated by subsite 1 interactions with the nonreducing end of the oligosaccharide substrate, minimizing nonproductive substrate binding. Through conformational changes, entropic contributions, and increased local concentration, subsite 2 subsequently has enhanced affinity for the second covalently linked glucosyl residue.

Glucoamylase (GA)[1] (1,4-α-D-glucan glucohydrolase, EC 3.2.1.3) is an exo-acting carbohydrase which cleaves D-glucose from the nonreducing ends of starch and related poly- and oligosaccharides. GA hydrolyses both α-1,4 and α-1,6 glucosidic linkages at a single catalytic site (*1*) with a nearly 400-fold preference for α-1,4 over α-1,6 linkages (*2*). The catalytic mechanism of GA is fairly flexible as both α-D-glucosyl fluoride (*3*) and *p*-nitrophenyl α-D-glucoside (*4*) can also be hydrolyzed.

The active site of GA has been modeled using a subsite theory (*5*). According to this theory, the substrate binding region of the enzyme can be depicted as a tandem array of modules (subsites) which interact with the monomer glucose units of the substrate. Steady-state kinetic studies of fungal GAs have indicated that the enzyme active site consists of about seven consecutive subsites, each of which can accommodate a glucosyl residue, with the catalytic site located between subsite 1 and subsite 2 (*2, 6, 7*). According to the subsite theory, substrates can bind to the enzyme in two different modes, either productive or nonproductive. In the productive mode (mode I, Figure 1), oligosaccharides have to occupy at least the first and the second subsites, thereby exposing the susceptible glycosidic linkage to the catalytic residues. Since GA is an exoenzyme with the catalytic site located between the first and second subsites, there is only one productive binding mode. Any binding of substrates which does not result in hydrolysis is termed a nonproductive mode (mode II, Figure 1).

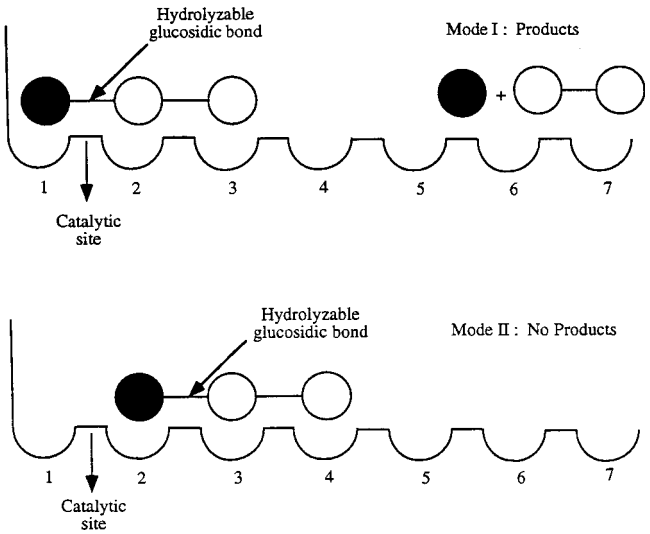

FIGURE 1: Schematic representation of glucoamylase subsites and illustration of productive and nonproductive binding modes according to the subsite model (*15*). Circles represent glucose units with the filled circle denoting the nonreducing end of the oligosaccharide.

Two carboxyl groups have been implicated in the GA hydrolytic mechanism (*8, 9*). Hydrolysis is postulated to

* Author to whom correspondence should be addressed. Tel: (410) 455-3403. Fax: (410) 455-1049.

‡ Present address: Department of Pathology, School of Medicine, Johns Hopkins University, Baltimore, MD 21205.

⊗ Abstract published in *Advance ACS Abstracts,* November 15, 1997.

[1] Abbreviations: GA, glucoamylase; GF, α-D-glucosyl fluoride.

S0006-2960(97)00820-9 CCC: $14.00

proceed by a general acid catalyst donating a hydrogen to the glucosidic bond oxygen and a catalytic base guiding the nucleophilic attack of a water molecule on the C-1 carbon of the aglycon moiety (*10*). Glu179 of *Aspergillus awamori* GA has been identified as the general acid catalyst (*11*) and Glu400 as the probable catalytic base group (*10, 12*−*14*).

The subsite model, as proposed (*15*), assumes a simple two-step mechanism for reactions in which the substrate is bound to the enzyme in the productive mode (eq 1). A one-

$$E + (G)_n \overset{K_{n,p}}{\Leftrightarrow} (EG)_{n,p} \xrightarrow{k_{int}} E + P \quad (1)$$

$$E + (G)_n \overset{K_{n,q}}{\Leftrightarrow} (EG)_{n,q} \quad (2)$$

step process is assumed to describe the substrate binding in the nonproductive mode (eq 2). On the basis of these assumptions, the GA reaction scheme can be written as follows where $(EG)_{n,p}$ and $(EG)_{n,q}$ represent the productive and nonproductive complexes respectively, between an *n*-mer oligosaccharide substrate $(G)_n$, and the enzyme; $K_{n,p}$ and $K_{n,q}$, the association constants for productive and nonproductive substrate binding respectively; and k_{int} represents the intrinsic hydrolytic rate constant. k_{int} is assumed to be the limiting rate of the reaction and is further assumed to be constant for all the productive complexes irrespective of the substrate length. The interaction between the subsite and the substrate residue gives rise to a decrease in free energy, or increase in affinity, which contributes to the binding of the substrate molecule as a whole to the active site. The "subsite affinity" for each subsite represents a quantitative characterization of the net strength of this specific interaction between the subsite and the substrate residue. The total affinity for the association of an *n*-mer substrate in a given binding mode is the sum of the affinities of all the subsites covered by the substrate in that mode of binding. The affinity of subsite *i* (numbered from the nonreducing end), A_i, for a given binding mode can be expressed as

$$\sum_{\text{covered subsites}}^{\text{over all}} A_i = RT \ln K_n + \Delta G_{mix} \quad (3)$$

where K_n is the association constant for that binding mode, *R* is the gas constant, *T* is the temperature, and ΔG_{mix}, equal to *RT* ln(solvent molarity), is the free energy difference arising from the solvent due to mixing independent of solute concentrations.

For a scheme described in eqs 1 and 2, the subsite affinities (A_i) are theoretically related to the steady-state kinetic parameters k_{cat} and K_m using eq 3. The subsite affinities are then calculated using experimentally determined k_{cat} and K_m. For GA, the values of k_{cat} increase and K_m decrease with increasing substrate length up to about seven glucosyl units (*2*). The ground-state affinities of the seven subsites have been calculated using this subsite model for GA from *Rhizopus delemar* at 25 °C (*15*) and for *Aspergillus awamori* at 50 °C (*2*) and at 8 °C [calculated using kinetic data from Olsen et al. (*16*)] and are given in Table 1. Subsite 1 has no or a small negative affinity, which has been attributed to subsite distortion to fit the nonreducing end of the substrate. Subsite 2 has the highest affinity among all the subsites, over 20 kJ/mol, while the affinities of the rest of the subsites, 3−7, decrease steadily with increasing distance from the catalytic site.

Table 1: Subsite Affinities[a] (kJ/mol) for Hydrolysis of Maltooligosaccharides by Glucoamylase at pH 4.5

	subsite affinities		
	R. delemar	*A awamori*	
subsite	at 25 °C[b]	at 50 °C[c]	at 8 °C[d]
1	0	−2.2	indeterminable
2	20.3	21.4	23.5
3	6.7	6.3	6.6
4	1.8	1.8	2.8
5	0.9	1.6	1.6
6	0.5	1.0	nd
7	0.4	0.3	nd

[a] Calculated using Hiromi's subsite affinity model (*15*). [b] From ref 15. [c] From ref 2. [d] Calculated using kinetic parameters from Olsen et al. (*16*). nd, not determined.

The subsite model makes several assumptions about the enzyme catalytic mechanism: first, bond hydrolysis is assumed to be the rate-limiting step of the reaction; second, only one enzyme−substrate intermediate is assumed to exist; third, the subsite affinities are assumed to be independent of each other; and fourth, the value for k_{int} is assumed to be constant regardless of substrate length. Several recent studies however have indicated that these assumptions may not be valid. The first assumption is not correct since product release has been shown to occur 4000-fold more slowly than bond hydrolysis (*17*). The second assumption is also not valid since both enzyme−substrate and enzyme−product complexes have been shown to exist (*17*). The third assumption is also questionable since the Trp120 loop region has a critical role in catalysis (*2, 18*) and undergoes conformational changes during the catalytic process (*19*) and spans several of the proposed distant subsites (*13, 14*), suggesting that the individual subsites are not independent of each other. The fourth assumption may also not be valid since kinetic parameters of *A. awamori* GA mutants, in particular Tyr116→Ala (*20*) and Arg122→Tyr GAs (*18*), have sharp irregularities in k_{cat} and K_m values with substrate lengths, suggesting a different catalytic mechanism for different substrate lengths. It is not possible to calculate subsite affinities for either Tyr116→Ala or Arg122→Tyr GAs assuming a constant hydrolytic rate using Hiromi's model. Since product release has recently been suggested as the rate-limiting step for GA hydrolysis (*17*), it is not surprising that k_{int} would vary with substrate length. Although these studies were performed using *Aspergillus* GAs, similar doubts about the assumptions of the subsite map arise with *Rhizopus* GAs since product release has also been suggested as a rate-limiting step (*3*) and transient kinetic studies indicate the presence of additional intermediates (*21*). Despite many similarities between *A. awamori* and *R. delamar* GAs not only in the primary amino acid sequence (*22*) but also in kinetic studies (*6, 16*), differences in their mechanisms seem to exist (*17*) and caution must be exercised in making any generalization for all GAs. Rather surprisingly, however, subsite affinities calculated for *R. delamar* and *A. awamori* GAs are very similar over a span from 8 to 50 °C (Table 1). The individual subsite affinities are relatively constant over a wide range of temperature, in contrast to what one would expect, as substrate binding improves significantly at lower temperatures (K_m for maltose

at 8 °C is about 10-fold lower than at 50 °C). The validity of the subsite map of *A. niger* GA has also been previously questioned (*23*). Since the assumptions in Hiromi's subsite model do not accurately reflect the kinetic behavior of wild-type and mutant GAs, the model is not applicable for GA and the GA subsite affinities calculated using this model hence are questionable.

In order to gain better insight into the subsite structure and substrate binding mechanism of GA, another approach must be used. Since both enzyme−substrate and enzyme−product intermediate complexes are present, steady-state data alone cannot provide information about enzyme−substrate binding and hence subsite affinities. Individual substrate association constants can be determined using pre-steady-state kinetics, and these values can be used to evaluate the affinity of each subsite. Glucose, a weak inhibitor of GA (*24*), binds to subsites 1 and/or 2 and binds more weakly than maltose. Subsite affinity maps of GA, calculated on the basis of Hiromi's theory for *A. awamori* and *R. delamar* GAs (Table 1), indicate that subsite 1 has little, if any, affinity for a glucosyl moiety in the enzyme−substrate complex while subsite 2 has an affinity around 20 kJ/mol (*2*, *7*, *15*), suggesting that glucose should predominantly bind to subsite 2. Individual association constants for glucose and maltose with GA can be determined by pre-steady-state kinetics and used to evaluate the individual affinities of subsites 1 and 2. This information can provide insight into the validity of the subsite theory and provide additional information into the GA substrate binding mechanism.

Recent stopped-flow spectrofluorometric studies have shown that substrate binding to the *A. awamori* GA active site is the primary factor in fluorescence quenching, although the ensuing hydrolytic step results in some additional quenching (*17*). Since glucose should bind to subsites 1 and/or 2 of GA, and given the high concentration of tryptophan residues around subsite 1 of GA (including Trp52, Trp178, Trp317, and Trp417) (*13*, *14*), a fluorescence signal associated with glucose binding is expected. Although, Tanaka et al. (*21*) had concluded the glucose interaction with *R. niveus* GA was too fast to be observed by stopped-flow techniques, preliminary results with *A. awamori* GA showed a detectable change in fluorescence. In this work, we carried out pre-steady state stopped-flow spectrofluorometry studies to probe the subsite interactions of wild-type *A. awamori* GA with glucose in H_2O and D_2O buffers. Studies were conducted in D_2O to investigate if the observable fluorescent signal from the glucose interaction with GA is for a "pure" binding process as opposed to the maltose interaction where signals were observed for both binding and hydrolysis. Solvent isotope effects observed using D_2O instead of H_2O are not expected to significantly affect pure weak binding interactions such as those predicted with glucose due to its high dissociation constant of 127 mM at 10 °C (*25*).

Steady-state kinetics using Trp120→Phe GA have shown that Trp120 plays a critical role in transition state stabilization (*2*) and product release for oligosaccharide substrates (*17*, *20*). Trp120 loop residues are also likely to be involved in substrate-induced conformational changes with oligosaccharides, based on the discrepancy between crystal structures and steady-state kinetic results (*18*). Here the Trp120→Phe GA interactions with maltose and glucose were studied to investigate whether Trp120 plays a role in substrate binding and to localize its possible involvement in substrate induced conformational changes.

MATERIALS AND METHODS

Materials. Wild-type and Trp120→Phe GA genes (*2*) were expressed in *Saccharomyces cerevisiae* and purified essentially as described (*18*). Ultrapure glucose (>99.5%), D_2O (99.9 atom % D) and acetic acid-*d* (CH_3COOD, 98 atom % D) were purchased from Sigma (St. Louis, MO).

Stopped-Flow Fluorescence Kinetics. The pre-steady-state kinetics of GA interactions with glucose were studied by monitoring the changes in the intrinsic enzyme fluorescence. The experiments were performed using a Hi-Tech scientific SF-61MX multimixing stopped-flow spectrofluorometer and analyzed essentially as described (*17*). The reaction mixture was excited at a wavelength of 280 nm, set using a monochromator. The emitted light was passed through a cutoff filter (WG320; 85% transmission at 320 nm) to resolve the fluorescence emission from the scattered incident light.

The kinetics of the wild-type interaction with glucose were studied in both H_2O and D_2O at 8 °C. The H_2O (pH 4.5) and D_2O (pD 5.0) buffers used were 0.05 M sodium acetate, and their methods of preparation are described elsewhere (*17*). The Trp120→Phe GA reactions with glucose or maltose were also performed at 8 °C in 0.05M sodium acetate buffer, pH 4.5. The temperature was maintained at 8.0 ± 0.1 °C with a circulating water bath. The final concentrations of both wild-type and Trp120→Phe GAs were 3 μM. Glucose concentrations up to 400 mM and maltose concentrations up to 15 mM were used in these studies. All the buffer, enzyme, and substrate solutions were filtered through a 0.45 μm filter before use. The substrate solutions were preincubated at 4 °C for at least 4 h to ensure anomeric equilibration. The dead time of the instrument was determined to be 1 ms under the experimental conditions. In each experiment at least 512 pairs of data were collected and a minimum of four such data sets were averaged for each substrate concentration. Each averaged set was fitted to analytical equations using nonlinear Gauss−Newton regression methods. Data analysis was performed with Hi-Tech rapid kinetics software.

RESULTS AND DISCUSSION

Glucose Binding to GA. Wild-type and Trp120→Phe GA interactions with glucose-quenched intrinsic fluorescence of the enzyme yielding typical stopped-flow traces as shown in Figure 2. Only one relaxation was observed and the data was best fit to a single exponential curve (eq 4)

$$f_t([G_1]) = A\alpha([G_1]) \exp(-k_{obs}t) + f_\infty([G_1]) \qquad (4)$$

where $f_t([G_1])$ represents the average molar fluorescence (i.e. total fluorescence/total number of moles) of all the enzyme species at glucose concentration $[G_1]$ and time t, k_{obs} is the first-order rate constant, $A\alpha([G_1])$ is the amplitude of the observable phase of the interaction, and $f_\infty([G_1])$ is the average molar steady-state fluorescence. Both the amplitude and the steady-state fluorescence are functions of substrate concentration. The amplitude is written as the product of a substrate concentration independent (A) and dependent (α) terms to facilitate fluorescence signal analysis.

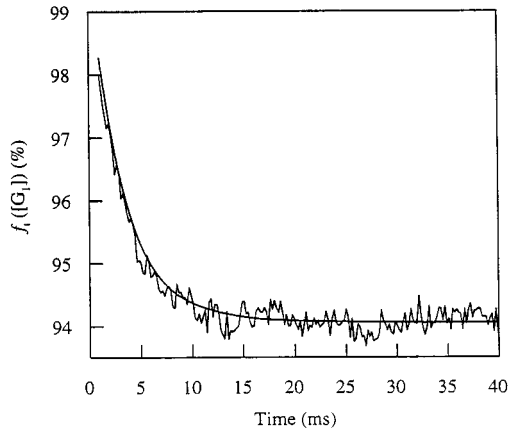

FIGURE 2: Typical time dependence of fluorescence changes during GA interaction with glucose. The signal illustrated here is obtained from wild-type GA (3 μM) reaction with glucose (100 mM) at 8 °C, pH 4.5. The signal above is an average of four traces. The average intrinsic fluorescence of the free enzyme is arbitrarily assigned a value 100%. The signal was fitted to a single exponential curve (eq 4).

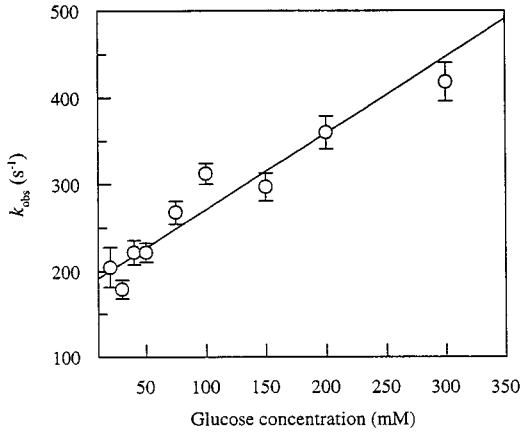

FIGURE 3: Concentration dependence of k_{obs} for glucose interaction with wild-type GA at 8 °C in H_2O buffer, pH 4.5. The line was obtained by fitting experimental data to the equation $k_{obs} = k_1[G_1] + k_{-1}$.

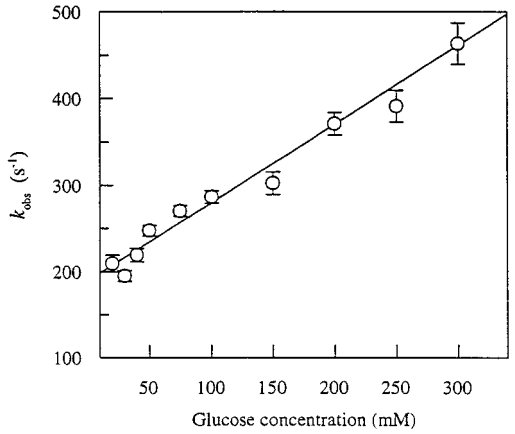

FIGURE 4: Concentration dependence of k_{obs} for glucose interaction with wild-type GA at 8 °C in D_2O buffer, pD 5.0. The line was obtained by fitting experimental data to the equation $k_{obs} = k_1[G_1] + k_{-1}$.

The concentration dependencies of the observed first-order rate constant, k_{obs}, of glucose interactions with wild-type GA in both H_2O (Figure 3) and D_2O (Figure 4) and with Trp120→Phe GA in H_2O (Figure 5) are linear. The linear dependence of k_{obs} on glucose concentration, [G_1], indicates

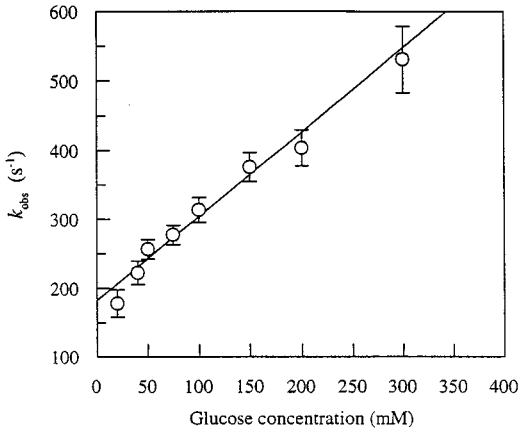

FIGURE 5: Dependence of k_{obs} on concentration for glucose interaction with Trp120→Phe GA in H_2O buffer, pH 4.5. The line is a fit of the experimental data to the equation $k_{obs} = k_1[G_1] + k_{-1}$.

that a single glucose molecule binds to GA in a one step reversible binding mechanism as shown in Scheme 1. The k_{obs} for such a mechanism is given by $k_{obs} = k_1[G_1] + k_{-1}$ (*26*).

Scheme 1

$$E + G_1 \underset{k_{-1}}{\overset{k_1}{\rightleftharpoons}} EG_1 \qquad K_1 = \frac{k_1}{k_{-1}}$$

The forward rate, k_1, and the reverse rate, k_{-1}, can be obtained as the slope and the intercept of such a linear plot between k_{obs} vs G_1. k_1 and k_{-1} for glucose interactions with wild-type GA in both H_2O and D_2O and with Trp120→Phe GA in H_2O are given in Table 2.

Careful analysis of the amount of fluorescence quenched and the amplitude of the signal provides valuable information about the individual fluorescence of the free and bound enzyme species. This information along with the rate of quenching data (k_{obs}) can be used to provide additional insight into the proposed reaction scheme. This analysis also provides an independent alternate route using steady-state fluorescence, f_∞, to calculate equilibrium constants to check the consistency of the model as demonstrated previously with the three-step mechanism proposed for GA and maltose (*17*).

The concentrations of both enzyme species, E and EG_1 in Scheme 1, can be obtained by solving enzyme mass balance equations and the individual rate equations and are given in eqs 5 and 6, respectively. In deriving these equations, the substrate concentration, [G_1], is assumed to be constant since it is in far excess of total enzyme concentrations. The substrate concentrations for all the glucose experiments were at least 500-fold higher than the enzyme concentrations used.

$$\frac{[E]}{[E_0]} = 1 - \alpha(1 - \exp(-k_{obs}t)) \tag{5}$$

$$\frac{[EG_1]}{[E_0]} = \alpha(1 - \exp(-k_{obs}t)) \tag{6}$$

where

Table 2: Pre-Steady-State Kinetic Results of the Wild-Type and Trp120→Phe GA Interactions with Glucose at 8 °C in H_2O or D_2O

	wild-type GA		Trp120→Phe GA
	H_2O[a]	D_2O[b]	H_2O[a]
k_1 (s^{-1} mM^{-1})	0.88 ± 0.13	0.91 ± 0.09	1.22 ± 0.10
k_{-1} (s^{-1})	183 ± 13	189 ± 8	182 ± 10
K_1[c] (mM^{-1})	0.0048 ± 0.0009	0.0048 ± 0.0006	0.0067 ± 0.0009
K_1[d] (mM^{-1})	0.0068 ± 0.0007	0.0064 ± 0.0008	0.0048 ± 0.0007
$(\Delta F_{EG_1})_{max}$ (%)	15.1 ± 0.7	17.1 ± 1.1	17.8 ± 1.9

[a] pH 4.5. [b] pD 5.0. [c] Calculated from individually determined k_1 and k_{-1}. [d] Calculated from steady-state fluorescence data values using eq 12.

$$\alpha = \frac{K_1[G_1]}{1 + K_1[G_1]} \quad (7)$$

The average fluorescence at any time t, f_t, can then be expressed as the sum of the fluorescence contribution of each enzyme species as follows

$$f_t = f_E\frac{[E]}{[E_0]} + f_{EG_1}\frac{[EG_1]}{[E_0]} \quad (8)$$

where f_E and f_{EG1} are molar fluorescences of E and EG_1, respectively. f_t can be written using the expressions for the concentrations (eqs 5 and 6) as

$$f_t = (f_E - f_{EG_1})\alpha \exp(-k_{obs}t) + (f_E(1 - \alpha) + f_{EG_1}\alpha) \quad (9)$$

Equation 9 is in the same form as eq 4 to which all the experimental data was fit. By comparing eqs 4 and 9, the amplitude of the fluorescence signal and the steady-state fluorescence, f_∞, can be expressed as in eqs 10 and 11, respectively:

$$\text{amplitude} = \alpha(f_E - f_{EG_1}) \quad (10)$$

$$f_\infty = f_E - \alpha(f_E - f_{EG_1}) \quad (11)$$

The fluorescence is quenched in glucose binding to GA (Figure 2), which indicates that the intrinsic fluorescence of the enzyme glucose complex, EG_1, is less than that of the free enzyme, E (i.e $(f_E - f_{EG1}) > 0$). α, as seen from eq 10, is a monotonically increasing function with glucose concentration. If $f_E > f_{EG1}$, the amplitude of the fluorescence signal resulting from Scheme 1 (eq 4) must increase with increasing glucose concentration, which is seen in the experimental data in the concentration range studied here. The amplitudes of the fluorescent signals observed with wild-type GA using 30 and 100 mM glucose are shown in Figure 6 as representative examples.

The steady-state fluorescence, f_∞, can be used to obtain the individual molar fluorescence of the involved enzyme species and the equilibrium constant K_1. The percentage of fluorescence quenched relative to the free enzyme when the system is at steady-state, $\Delta F_\infty([G_1])$, can be experimentally determined at various glucose concentrations and can be written using the expression for f_∞ from eq 11 as

$$\Delta F_\infty([G_1]) = \frac{f_E - f_\infty}{f_E} \times 100\% = \frac{(\Delta F_{EG_1})_{max}[G_1]}{\frac{1}{K_1} + [G_1]} \quad (12)$$

where $(\Delta F_{EG1})_{max}$ is the percentage difference in the molar fluorescence of EG_1 relative to E. According to eq 12, ΔF_∞ should have an hyberbolic dependence on $[G_1]$ which is the case for glucose interactions with both wild-type and the mutant enzymes. ΔF_∞ vs $[G_1]$ for wild-type/glucose binding is shown in Figure 7 as a typical example. $(\Delta F_{EG1})_{max}$ and K_1 can be determined by fitting ΔF_∞ vs $[G_1]$ to eq 12, and the values thus calculated for glucose interactions with wild-type GA in H_2O and D_2O and Trp120→Phe GA in H_2O are given in Table 2.

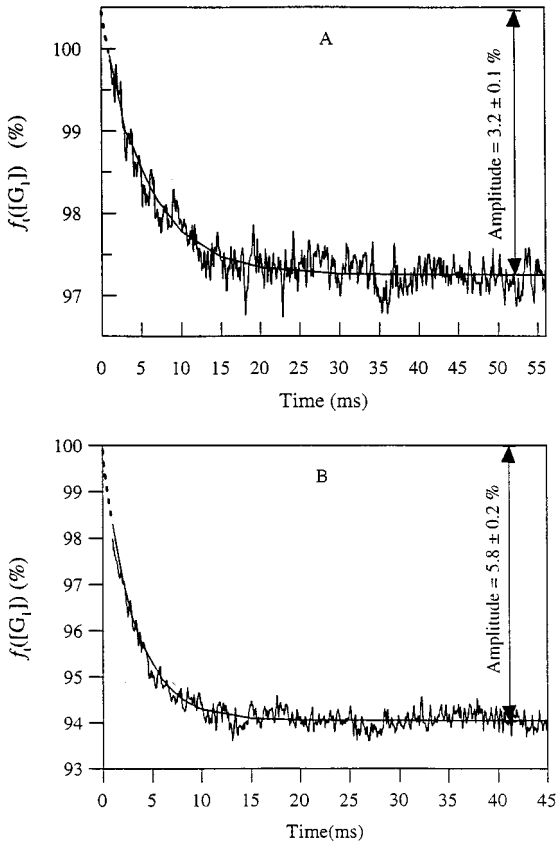

FIGURE 6: Illustration of the increase in amplitude of the observed fluorescence signal with increasing substrate concentration for GA interactions with glucose. The amplitudes of the fluorescence signal in the wild-type GA (3 μM) at glucose concentrations of (A) 30 mM and (B) 100 mM are shown here as examples. The magnitude of the molar fluorescence of the system are all relative to that of the free enzyme (100%). The curves are a fit of the stopped-flow traces to eq 4, with the solid curve representing the fit to the experimentally observed signal and the dotted curve representing the interpolation of the data between 0 and 1 ms (dead time). The amplitude, $A[G_x]\alpha$, is as defined in eq 4, and is simply equal to the difference in the intrinsic fluorescence at times $t = 0$ and $t = \infty$ [or at times at which $\exp(-k_{obs}t)$ is negligible].

The association (k_1) and dissociation (k_{-1}) rate constants given in Table 2 for the wild-type GA/glucose interaction in H_2O indicate that glucose binds very weakly to the active site. Typical association rate constants for enzyme−substrate interactions are in the range of 10^6−10^8 M^{-1} s^{-1} at room

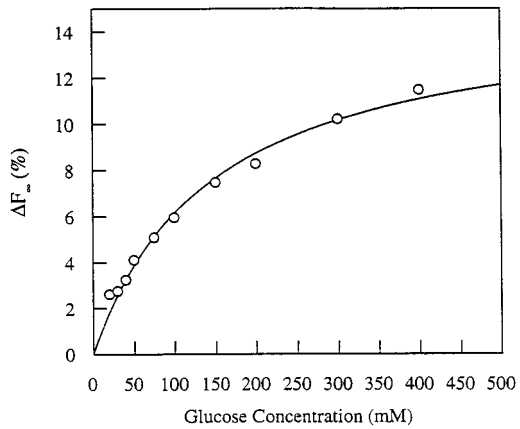

FIGURE 7: Fluorescence quenched when glucose binding to wild-type GA reaches a steady-state, ΔF_∞, plotted against glucose concentration. The average intrinsic fluorescence of the system at steady-state, f_∞ (eq 4), is subtracted from that of the free enzyme (100%) to obtain ΔF_∞. The curve is a fit to the experimental values of ΔF_∞ to eq 12. Relative standard deviation for ΔF_∞ data, ±1%.

temperature (*27*), so the very low calculated k_1 value of 8.8 $\times$ 10^2 M^{-1} s^{-1} at 8 °C for glucose is indicative of poor binding. The association equilibrium constant for glucose is 4.8 M^{-1} ($K_1 = k_1/k_{-1}$ calculated from the individual rate constants; Table 2). This value calculated using pre-steady-state experiments is similar to that obtained for glucose binding to *R. niveus* GA (7.9 M^{-1} at 10 °C) using steady-state fluorometric experiments (*25*). Glucose binding is also shown to be very weak when compared to the association constant of 9.4 $\times$ 10^{11} M^{-1} for acarbose, a potent GA inhibitor (*28*), and 120 M^{-1} for the substrate maltose (*17*). The rate constants and fluorescence data thus all suggest a simple weak glucose binding to GA as proposed in Scheme 1.

The k_1 and k_{-1} values obtained for the wild-type GA/glucose interaction in D_2O (Table 2) are identical to the values obtained in H_2O, indicating the absence of any solvent isotope effects. This absence of an isotopic effect further suggests that the glucose interaction with wild-type GA represents a simple weak binding step. A significant isotopic effect was observed on the maltose binding step with GA, resulting in a nearly 2-fold increase in K_1. This increase was attributed to the extensive hydrogen-bonding network involved in the specific ground-state binding of maltose (*17*). These results are consistent with the GA crystal structure, which shows a preponderance of hydrophobic residues around subsite 1 and several residues which may contribute charged or uncharged hydrogen bonds in subsite 2 (*13*, *14*). Therefore a lack of an isotopic effect for glucose, which initially binds weakly to the hydrophobic pocket of subsite 1, and an isotopic effect for maltose, which binds at subsite 2 via specific hydrogen bonds, are reasonable. The k_1 and k_{-1} values obtained for the glucose interaction with Trp120→Phe GA in H_2O (Table 2) are also very similar to those obtained with the wild-type, indicating that glucose binds similarly to the mutant in a weak association step and that Trp120 plays no direct role in glucose binding.

The $(\Delta F_{EG1})_{max}$ (Table 2) calculated using steady-state fluorescence values provides more information about the nature of the glucose interactions with the active site. The $(\Delta F_{EG1})_{max}$ value of 15.1% for wild-type GA/glucose binding in H_2O indicates that the fluorescence of an enzyme−glucose complex molecule is 15.1 % less than that of a free enzyme molecule. The $(\Delta F_{EG1})_{max}$ value for glucose binding to wild-type GA in D_2O (Table 3) is 17.2%. Recent studies have shown that the fluorescence of the wild type GA−maltose complex is about 16.2% less than that of the free enzyme in H_2O and about 19.9% less in D_2O (*17*). The similar fluorescence quenching values of GA−maltose and GA−glucose complexes in both H_2O and D_2O suggest that the complexes involved are also similar. The fluorescence signal resulting from glucose binding should therefore be a result of binding only to the first or the second subsite, even though the GA active site contains seven subsites each capable of accommodating a glucosyl unit.

A number of independent observations are available suggesting glucose binds at subsite 1 of GA. First, crystallographic structures (*12*−*14*, *29*, *30*) strongly suggest the fluorescence signal associated with maltose binding likely results from a subsite 1 interaction since most active site tryptophans are clustered around subsite 1, including Trp52, Trp178, Trp317, and Trp417. Similar fluorescence intensities of glucose and maltose complexes (Table 2) suggest that glucose binds to subsite 1. Second, crystal structures of GA−acarbose and GA−D-*gluco*-dihydroacarbose, at both pH 4.0 and 6.0, show that the inhibitors bind only in forms where subsite 1 is clearly occupied (*30*). The GA−1-deoxynojirimycin structure (*12*) also shows the inhibitor predominantly bound to subsite 1 with very low occupancy at subsite 2. Third, a single reaction scheme including only a productive hydrolytic step agrees very well with pre-steady-state and steady-state kinetic data (*17*), arguing against the presence of any significant nonproductive binding and indicating little, if any, substrate binding not involving subsite 1. Fourth, part of the basis for Hiromi's nonproductive binding model came from studies on lysozyme where the crystal structure indicated nonproductive substrate binding. However, none of the available crystal structures of GA indicate appreciable nonproductive binding as would be expected with a dominant subsite 2 affinity. Fifth, since condensation reactions occur at high glucose concentrations, the first glucose molecule must bind at subsite 1, since that subsite is inaccessible after subsite 2 is occupied. Sixth, modeling of pre-steady-state kinetic parameters obtained with maltose using both productive and nonproductive binding reaction schemes indicated that nonproductive binding did not occur significantly and that subsite 1 affinities need to be reevalutated (*23*). Finally, preliminary presteady state results obtained for the hydrolysis of glucosyl fluoride which must bind at subsite 1, indicate a similar fluorescence signal to that expected with α-glucose.

Individual Subsite Affinities. The subsite affinities of GA as calculated with the steady-state kinetic parameters using the Hiromi model, in particular the affinities of subsites 1 and 2, are very questionable due to the invalid assumptions required for the model. An alternative procedure is to utilize pre-steady-state kinetics to determine substrate association equilibrium constants for different ligands and to use these values to calculate the ground-state affinities of the individual subsites. The association constants, K_1, for the glucose/wild-type reaction in H_2O and D_2O have been obtained here (Table 2) and for maltose/wild-type GA binding are known (*17*). These values can be compared to estimate the affinities of subsites 1 and 2 for wild-type GA.

The role of Trp120 in substrate binding to subsites 1 and 2 can be elucidated by comparing the association constants for glucose and maltose and the resultant subsite affinities

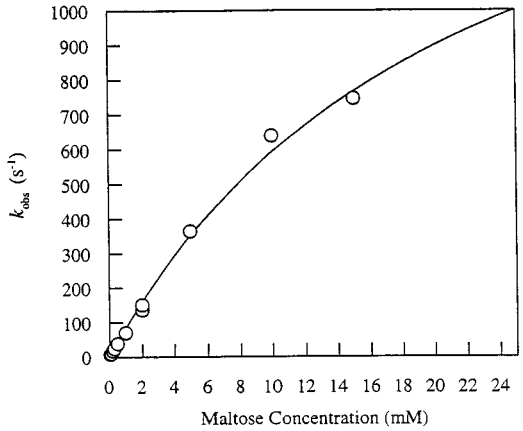

FIGURE 8: Dependence of the observed first-order rate constant, k_{obs}, on substrate concentration for the Trp120→Phe GA reaction with maltose at 8 °C, pH 4.5. The curve was obtained by fitting experimental data to a hyperbolic equation as described (*17*).

Table 3: Pre-Steady-State Kinetic Results of the Wild-Type and Trp120→Phe GA Reactions with Maltose at 8 °C, pH 4.5

	wild-type[a]	Trp120→Phe
K_1 (mM^{-1})	0.12 ± 0.01	0.047 ± 0.009
k_2 (s^{-1})	1392 ± 68	1849 ± 236
k_{-2} (s^{-1})	31.7 ± 1.9	3.6 ± 0.4
ΔF_{max} (%)	20.6 ± 0.4	18.6 ± 0.4

[a] From ref 17.

for both wild-type and Trp120→Phe GA. The association constant of Trp120→Phe GA with glucose is given here and with maltose has been previously reported (*16*). However our repeated stopped-flow experiments studying the Trp120→Phe GA/maltose reaction gave k_{obs} values at moderate to high substrate concentrations (≥5mM) that differed significantly from the earlier reported data. We therefore report the rate constants we obtained for the Trp120→Phe GA/maltose reaction here. The dependence of k_{obs} on maltose concentration is shown in Figure 8. The fluorescence quenching observed in the maltose reaction with Trp120→Phe GA (data not shown) indicates a two-step process similar to that seen with wild-type GA, and the individual rate constants were determined as described previously (*17*). The rate constants, K_1, k_2, and k_{-2} obtained are given in Table 3 along with the corresponding values previously obtained with wild-type GA for comparison. Compared to wild-type, the Trp120→Phe mutant decreases the K_1 value about 2.5-fold for maltose binding, but the value is unchanged for glucose binding, indicating an unfavorable effect on binding at subsite 2. This decrease in substrate complex formation with the mutant enzyme indicates that the decreased K_m value obtained from steady-state studies with maltose (*2*) reflects an increase in product complex formation, reaffirming the role of the Trp120 region in the product release step. The k_{-2} and ΔF_{max} (total fluorescence quenched) values obtained here are similar to those reported previously (*16*).

The equilibrium constants, K_1, can now be used to determine subsite 1 and 2 affinities for wild-type and Trp120→Phe GAs. Since D-glucose exists in solution as a mixture of α and β anomers (α:β, 36:64), either form can potentially bind as the substrate. With maltose, however, only the α-form of the nonreducing end glucose is present to bind to subsite 1 in a productive complex. In order to obtain an estimate of subsite affinities comparing the binding constants of glucose and maltose, the affinity of the α-anomer should be evaluated. The α-anomer is expected to bind significantly better than the β-anomer for three reasons. First, GA cleaves α-linked and not β-linked substrates and generates β-D-glucose as a product. Crystallographic evidence (*12*) indicates that the attacking nucleophilic water in hydrolysis, water500 (hydrogen bonded to Glu400), will have to be displaced from the active site in order for the β-anomer of glucose or glucose analogs to bind. However, no such steric conflict would exist between water500 and the α-anomer of glucose and glucose analogs. It makes inherent sense for the enzyme to have developed, through evolution, a mechanism to bind the α-linked substrates differently from the β-anomeric product. Second, equilibrium dissociation constants suggest that α-GF binds much better than the mixed anomers of glucose. The respective dissociation constants for α-GF and glucose with *A. awamori* GA are 17.5 mM (*17*) and 208 mM ($1/K_1$ from Table 2) at 8 °C and with *R. niveus* GA are 25 mM at 25 °C (*3*) and 127 mM at 10 °C (*25*). Third, stopped-flow experiments show that α-GF quenches GA fluorescence 2.5−3.0-fold more than mixed-anomeric glucose at similar concentrations (Natarajan and Sierks, unpublished observations).

In order to account for the possible differences in binding affinities of α and β anomers at subsite 1, we can write the affinity of subsite 1 as

$$A_1 = A_{1\alpha}\left(\frac{\alpha}{\alpha+\beta}\right) + A_{1\beta}\left(\frac{\beta}{\alpha+\beta}\right) \quad (13)$$

where $A_{1\alpha}$ is the affinity for α-anomer, $A_{1\beta}$ is the affinity for β-anomer, and α and β are the relative amounts of α- and β-anomers, respectively, at equilibrium. Though the actual preference for α-anomer cannot be quantified with the available data, the following two limiting cases provide reasonable limits to the subsite affinities. The first case assumes that affinities for both anomers are equal. So eq 13 becomes

$$A_1 = A_{1\alpha} = A_{1\beta} \quad (14a)$$

The second case assumes that the β-anomer has no affinity. So eq 13, in this case, can be written as

$$A_1 = A_{1\alpha}\left(\frac{\alpha}{\alpha+\beta}\right) \quad (14b)$$

The free energy for glucose association, $\Delta G_{(Glucose)} = (-RT \ln (K_1)_{Glucose})$ can be related to subsite affinity using eq 3 as

$$A_1 = RT \ln (K_1)_{Glucose} + \Delta G_{mix} \quad (15)$$

Using approximations of eqs 14a and 14b, eq 15 can be written respectively in a rearranged form as

$$A_{1\alpha} = RT \ln (K_1)_{glucose} + \Delta G_{mix}, \quad \text{assuming} \quad A_{1\alpha} = A_{1\beta} \quad (16a)$$

$$A_{1\alpha}\left(\frac{\alpha}{\alpha+\beta}\right) = RT \ln (K_1)_{glucose} + \Delta G_{mix}, \quad \text{assuming} \quad A_{1\beta} = 0 \quad (16b)$$

The free energy change for maltose association, $\Delta G_{(Maltose)} = (-RT \ln (K_1)_{Maltose})$ can be related to subsite affinities using

Table 4: Subsite Affinities of *A. awamori* Glucoamylase at 8 °C in kJ/mol

enzyme (solvent)	subsite 1 affinity for α-glucose	subsite 2 affinity
wild-type (H_2O)	13.0[a]	7.5[a]
	36.2[b]	−15.7[b]
wild-type (D_2O)	12.8[a]	9.8[a]
	35.6[b]	−13.0[b]
Trp120→Phe (H_2O)	13.8[a]	4.7[a]
	38.4[b]	−20.0[b]

[a] Calculated by solving eqs 16a and 17 simultaneously; Assumes α- and β-glucose have same affinity for subsite 1. [b] Calculated by solving eqs 16b and 17 simultaneously; Assumes β-glucose has no affinity for subsite 1.

eq 3 as

$$A_{1\alpha} + A_2 = RT \ln (K_1)_{\text{Maltose}} + \Delta G_{\text{mix}} \qquad (17)$$

$A_{1\alpha}$ determined form eqs 16a and 16b can be substituted in eq 17 to obtain A_2 for the two limiting cases discussed. The resulting values of $A_{1\alpha}$ and A_2 for wild-type and Trp120→Phe GA are given in Table 4.

The subsite 1 affinity for wild-type GA in H_2O at 8 °C thus calculated is between 13 and 36 kJ/mol, depending on the extent of the preference for α-anomer over β-anomer. The apparent subsite 2 affinity is estimated to be between −15.7 and 7.5 kJ/mol. The suggested substrate-induced conformational changes (*18*) likely revolve around subsite 2 in the enzyme−substrate complex (discussed later) and hence the apparent subsite 2 affinity includes the energy expended by the enzyme to accommodate the substrate at subsite 2 or any strain in the substrate to bind to both subsite 1 and subsite 2. The affinities and binding energetics obtained here conflict with Hiromi's model, wherein a negative or indeterminable subsite 1 affinity was often obtained, suggesting the low subsite 1 affinity included the energy required for the distortion of subsite 1. Here we show that the affinity of subsite 1 is higher than subsite 2 in either of the two limiting cases discussed, consistent with subsite 1 being the primary binding site. Although the range of values presented here for subsite affinities is admittedly large, these values more accurately reflect the many experimental observations made with GA than Hiromi's model does, and they qualitatively provide a different mechanism for GA activity.

The subsite 1 affinity is also not affected by solvent isotope. As discussed earlier, the absence of an isotopic effect on glucose binding is reflected in a similar absence of an effect on the subsite 1 affinity, presumably due to the somewhat nonspecific nature of the hydrophobic binding pocket containing several tryptophan residues which comprise subsite 1. A lack of an isotope effect on the K_1 value suggests that the proposed hydrogen-bond interactions in subsite 1, between Arg54 and Asp55 and the 4-OH and 6-OH groups of the glucose unit in subsite 1 (*13, 14*), are not completely realized during the initial substrate complex formation, but rather, these bonds achieve their maximum strength in the transition state for bond hydrolysis. Previous evidence for hydrogen bonding in subsite 1 playing a role in transition-state stabilization rather than ground-state substrate binding was obtained in steady-state experiments using mutations at Asp55 (*33*) and Arg54 (*34*). The subsite 2 affinity does show a solvent isotope effect suggesting that hydrogen bonds are involved in the enzyme/substrate ground state complex, again in agreement with steady-state studies on GA mutants which indicated Glu180 forms a charged hydrogen bond (*11*) with the 2-OH group of the glucose unit in the second subsite (*32*), and that this bond strongly influences ground state binding.

Binding studies with glucose indicate that the subsite 1 affinity is also not affected by the Trp120→Phe mutation. This is consistent with Trp120→Phe mutation having no significant effect on binding and hydrolysis of GF, which has to bind to subsite 1 for catalysis (*17*). However the affinity of subsite 2 is about 3−4 kJ/mol lower in Trp120→Phe GA compared to wild-type GA (Table 4), depending on the preference for α-anomer in subsite 1. Presumably Trp120 plays an important role in substrate binding at subsite 2 and mutation of this residue affects this interaction. Trp120 has been suggested to play a role in substrate-induced conformational changes, and here we show these changes occur away from subsite 1. Although the experiments in this work are directly related only to the subsites 1 and 2, it is very likely that Trp120→Phe mutation also affects the more distant subsites.

Substrate Binding Mechanism. This information on the subsite affinities and binding rates of GA provides new insights into the GA substrate binding mechanism. Two theories have previously been proposed to explain the binding of oligosaccharides to the subsites of glucoamylase. Both of these theories are primarily based on the high affinity of subsite 2 (19−23 kJ/mol for GAs from different organisms (*2, 7, 15, 35*) as determined using Hiromi's model. Tanaka and coworkers (*21, 36*) have suggested that the nonreducing end of the substrate first binds to subsite 2 and then slowly relocates to subsite 1 (Figure 9A). Fagerström (*35*) suggested that it is also likely that the penultimate glucose moiety of the substrate (from the nonreducing end) first binds to subsite 2 to form a loose complex and later the enzyme undergoes conformational changes to form a more stable subsite 1, which results in a tighter complex (Figure 9B). Since the subsite model derived by Hiromi is not valid for *A. awamori* GA and is likely not valid for other GAs as well, these binding models need to be reinterpreted.

We propose a substrate binding mechanism, which is different from the ones outlined above, based on the pre-steady-state results for the glucose interaction, along with the three-step mechanism described for oligosaccharides (*17*), indirect evidence for substrate induced conformational changes (*18*), existing data from steady-state analysis of GA mutants, and the known GA crystal structures. The nonreducing end of the oligosaccharide substrate first binds to subsite 1. Upon initial binding at subsite 1, the affinity of subsite 2 is enhanced through several mechanisms, including an expected increase in effective concentration of the glucose unit in subsite 2 (*37*), an associated decrease in entropy loss of the disaccharide binding to subsites 1 and 2 relative to two monosaccharides, and an accompanying conformational change to enhance binding at subsite 2 and more distant subsites (Figure 9C). The Trp120 loop residues, and Trp120 in particular, plays an important role in the substrate-induced conformational changes around subsite 2. Presumably, it is these conformational changes around subsite 2 which are reversed during the rate-limiting slow release of the reducing end from subsite 2.

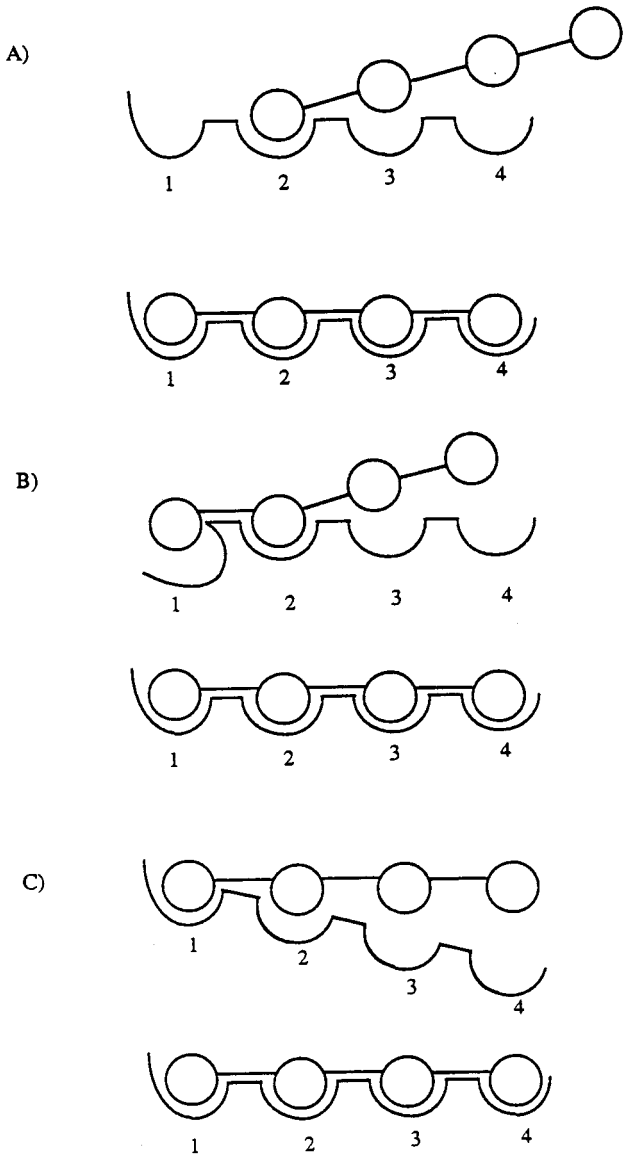

FIGURE 9: (A) Schematic drawing of the proposed GA binding mechanism (*36*) showing an initial fast recognition step of substrate to subsite 2 followed by a unimolecular rearrangement to the active configuration. (B) Schematic drawing of the second proposed GA binding mechanism (*35*) showing an initial fast recognition step of substrate primarily driven by the high affinity of subsite 2 of GA followed by a conformational change at subsite 1 to obtain the active configuration. C) Our proposed GA binding mechanism showing primary binding at subsite 1 accompanied by conformational changes and an increase in effective concentration which enhance the affinity of subsite 2 and the adjoining subsites to form stable subsites.

Significant differences in binding of the monomer glucose and dimer maltose to GA indicate that the whole is greater than the sum of the parts. While glucose binding is weak (low K_1) and slow (low k_1) enough to be observed by stopped-flow techniques, maltose binding is substantially stronger (25-fold higher K_1) and too fast to be monitored (*17*). Although these observations suggest that the second glucose unit in maltose binds to GA much better than the first unit, the binding itself seems to be initiated by the first unit binding to subsite 1. Many instances exist where individual molecules (say A and B) have weak or negligible binding to biological molecules, while the covalently linked molecule (A−B) has significantly higher affinity, as discussed in a review by Jencks (*37*).

CONCLUSION

A single glucose weakly binds to GA, under the conditions studied, in a single step reversible mechanism, $E + G_1 \leftrightarrow EG_1$, quenching the enzyme fluorescence in the process. A number of different lines of reasoning, including similar fluorescence intensities of the GA−maltose and GA−glucose complexes, the high concentration of tryptophans around subsite 1, several crystal structures of GA−inhibitor complexes, pre-steady-state and steady-state kinetic modeling, occurrence of condensation reactions, and similar binding characteristics of glucose and α-glucosyl fluoride, all taken together, strongly suggest that glucose binds at subsite 1. The Trp120 residue does not play a role in this glucose recognition at subsite 1, although it does play a role in subsite 2 binding and product release. The subsite affinitiy map originally proposed by Hiromi was calculated from steady state kinetic data. Information about substrate binding cannot be obtained from steady-state data where contributions from enzyme−substrate and enzyme−product complexes are often inseparably mixed. Recent steady-state and pre-steady-state kinetic studies have indicated that there are also several other questionable assumptions in the proposed mechanism. A new method of calculating subsite affinities is needed. Here we show that the affinities of subsites 1 and 2 of GA can be calculated using the substrate association constants of glucose and maltose from pre-steady-state experiments. Our results indicate that subsite 1 has significantly higher affinity than subsite 2 in the enzyme ground state, in contrast to the results obtained with the previous model. This new subsite affinity map of GA is consistent with other available evidence, suggesting that substrate binding is initiated through subsite 1 interactions. The mechanism proposed here is also more satisfying from an evolutionary perspective, since reducing nonproductive binding increases enzyme efficiency, suggesting that GA is not as primitive as previously believed.

REFERENCES

1. Hiromi, K., Kawai, M., and Ono, S. (1966) *J. Biochem. 59*, 476−480.
2. Sierks, M. R., Ford, C., Reilly, P. J., and Svensson, B. (1989) *Protein Eng. 2*, 621−625.
3. Kitahata, S., Brewer, C. F., Genghof, D. S., Sawai, T., and Hehre, E. J. (1981) *J. Biol. Chem. 256*, 6017−6026.
4. Selwood, T., and Sinnott, M. L. (1990) *Molecular Mechanisms in Biorganic Processes* (Golding, B. T., and Bleasdale, C., Eds.) Royal Society of Chemistry, Cambridge.
5. Hiromi, K. (1970) *Biochem. Biophys. Res. Commun. 40*, 1−6.
6. Hiromi, K., Ohnishi, M., and Tanaka, A. (1983) *Mol. Cell. Biochem. 51*, 79−85.
7. Meagher, M. M., Nikolov, Z. L., and Reilly, P. J. (1989) *Biotech. Bioeng. 34*, 681−688.
8. Hiromi, K., Takahashi, K., Hamauzu, Z., and Ono, S. (1966) *J. Biochem. 59*, 476−480.
9. Savel'ev, A. N., and Firsov, L. M. (1982) *Biochemistry (USSR)*, 47, 1365−1367.
10. Frandsen, T. P., Dupont, C., Lehmbeck, J., Stoffer, B., Sierks, M. R., Honzatko, R., and Svensson, B. (1994) *Biochemistry 33*, 13808−13816.
11. Sierks, M. R., Ford, C., Reilly, P. J., and Svensson, B. (1990) *Protein Eng. 3*, 193−198.
12. Harris, E. M. S, Aleshin, A. E., Firsov, L. M., and Honzatko, R. B. (1993) *Biochemistry 32*, 1618−1626.
13. Aleshin, A. E., Hoffman, C., Firsov, L. M., and Honzatko, R. B. (1994) *J. Mol. Biol. 238*, 575−591.
14. Aleshin, A. E., Firsov, L. M., and Honzatko, R. B. (1994) *J. Biol. Chem. 269*, 15631−15639.

15. Hiromi, K. (1972) *Proteins: Structure and Function*, (Funatsu, M., Hiromi, K., Imahori, K., Murachi, T., and Narita, K., Eds. Vol. 2, pp 1−46, Halsted Press, New York.
16. Olsen, K., Christensen, U., Sierks, M. R., and Svensson, B. (1993) *Biochemistry 32*, 9686−9693.
17. Natarajan, S. K., and Sierks, M. R. (1996) *Biochemistry 35*, 15269−15279.
18. Natarajan, S. K., and Sierks, M. R. (1996) *Biochemistry 35*, 3050−3058.
19. Svensson, B., and Sierks, M. R. (1992) *Carbohydr. Res.* 227, 29−44.
20. Sierks, M. R., and Svensson, B. (1996) *Biochemistry 35*, 1865−1871.
21. Tanaka, A., Ohnishi, M., and Hiromi, K. (1982) *Biochemistry 21*, 107−113.
22. Itoh, T., Ohtsuki, I., Yamashita, I., and Fukui, S. (1987) *J. Bacteriol.* 169, 4171−4176.
23. Christensen, U., Olsen, K., Stoffer, B. B., and Svensson, B. (1996) *Biochemistry* 35, 15009−15018.
24. Hiromi, K., Kawai, M., Suetsugu, N., Nitta, Y., Hosotani, T., Nagao, A., Nakajima, T., and Ono, S. (1973) *J. Biochem.74*, 935−943.
25. Hiromi, K., Tanaka, A., and Ohnishi, M (1982) *Biochemistry 21,* 102−107.
26. Bagshaw, C. R., Eccleston, J. F., Eckstein, F., Goody, R. S., Gutfreund, H., and Trentham, D. R. (1974) *Biochem. J. 141*, 351−364.
27. Fersht, A. (1985) *Enzyme Structure and Mechanism*, 2nd ed., W. H. Freeman, New York.
28. Berland, C. R., Sigurskjold, B. W., Stoffer, B., Frandsen, T. P., and Svensson, B. (1995) *Biochemistry* 34, 10153−10161.
29. Stoffer, B., Aleshin, A. E., Firsov, L. M., Svensson, B., and Honzatko, R. B. (1995) *FEBS Lett. 358*, 57−61.
30. Aleshin, A. E., Stoffer, B., Firsov, L. M., Svensson, B., and Honzatko, R. B. (1996) *Biochemistry 35*, 8319−8328.
31. Sierks, M. R., and Svensson, B. (1992) *Protein Eng.* 5, 185−188.
32. Sierks, M. R. Bock, K, Refn, S., and Svensson, B. (1992) *Biochemistry 15*, 8972−8977.
33. Sierks, M. R., and Svensson, B. (1993) *Biochemistry 32*, 1113−1117.
34. Frandsen, T. P., Christensen, T., Stoffer, D., Lehmbeck, J., Dupont, C., Honzatko, R and Svensson, B. (1995) *Biochemistry 34*, 10162−10169.
35. Fagerström, R. (1991) *J. Gen. Microbiol. 137*, 1001−1008.
36. Tanaka, A., Yamashita, T., Ohnishi, M., and Hiromi, K. (1983) *J. Biochemistry 93*, 1037−1043.
37. Jencks, W. P. (1981) *Proc. Natl. Acad. Sci., U.S.A. 51*, 79−85.

BI970820X